ASSESSING NITROGEN CONTENT IN FLOOD-IRRIGATED RICE PLANTATIONS USING UAV-BASED MULTISPECTRAL IMAGERIES

Gabriella Santos Arruda de Lima[1]
Manuel Eduardo Ferreira[2]
Maik Leão dos Santos[3]
Alexandre Bryan Heinemann[4]
João Vitor Silva Costa[5]

ABSTRACT

Nitrogen is essential for agricultural crops, especially rice, and monitoring its demand is crucial. Remote sensing offers a fast and efficient alternative to field sampling, facilitating fertilizer management. This study estimated agronomic parameters related to nitrogen status in flooded rice, total above-ground biomass (AGB), leaf nitrogen content (LNC), leaf area index (LAI), and productivity, using a multispectral UAV sensor and a proximal optical reflectance sensor (Crop Circle), compared to traditional sampling in experimental plots. Simple and multiple linear regressions were applied. Field sensor data achieved coefficients of determination (R^2) of 0.89 and 0.85 for LNC and LAI, respectively. The growing stage significantly affected the performance of vegetation indices, whereas rice variety had no significant impact. Model performance varied with phenological stage, with AGB, LNC, and LAI best estimated during the reproductive stage, and yield during grain filling. Effective results were also obtained when combining all stages. UAV-based analysis proved a promising alternative, overcoming satellite cloud cover limitations, offering high cartographic accuracy, historical records over larger areas, and shorter operational time compared to field optical sensors and traditional methods.

Keywords: Unmanned Aerial Vehicle (UAV); nutrient utilization efficiency; vegetation indices; rice.

AVALIAÇÃO DO TEOR DE NITROGÊNIO EM PLANTAÇÕES DE ARROZ IRRIGADAS POR INUNDAÇÃO USANDO IMAGENS MULTIESPECTRAIS BASEADAS EM VANT

RESUMO

O nitrogênio é essencial para culturas agrícolas, especialmente o arroz, sendo fundamental monitorar sua demanda. O sensoriamento remoto oferece uma alternativa rápida e eficiente ao monitoramento de campo, facilitando o manejo da adubação. Este estudo estimou parâmetros agronômicos relacionados ao estado de nitrogênio no arroz irrigado, biomassa aérea total (AGB), teor de nitrogênio foliar (LNC), índice de área foliar (LAI) e produtividade,

[1]Doutora em Geografia, pesquisadora da Universidade Federal de Goiás (UFG)/LAPIG, Goiânia-GO, Brasil; e-mail: gabriella.arruda.lima@gmail.com
[2]Doutor em Ciência Ambientais, Professor da Universidade Federal de Goiás (UFG)/LAPIG, Goiânia-GO, Brasil; e-mail: manuel@ufg.br
[3]Doutorando em Fitopatologia, Universidade Federal de Viçosa (UFV), Viçosa-MG, Brasil; e-mail: maik.santos@ufv.br
[4]Doutor em Agronomia, pesquisador na Embrapa Arroz e Feijão, Santo Antônio de Goiás-GO, Brasil; e-mail: alexandre.heinemann@embrapa.br
[5]Mestre em Ciências Ambientais, Universidade Federal de Goiás (UFG)/LAPIG, Goiânia-GO, Brasil; e-mail: joao_vitor@discente.ufg.br

utilizando um sensor multiespectral embarcado em VANT e um sensor óptico proximal (Crop Circle), comparados a amostragens tradicionais em parcelas experimentais. Foram aplicadas regressões lineares simples e múltiplas. Os dados obtidos pelo sensor de campo apresentaram coeficientes de determinação (R^2) de 0,89 e 0,85 para LNC e LAI, respectivamente. O estágio de crescimento influenciou significativamente o desempenho dos índices de vegetação, enquanto a variedade de arroz não apresentou efeito relevante. O desempenho dos modelos variou conforme o estágio fenológico, sendo AGB, LNC e LAI mais precisamente estimados no estágio reprodutivo, e a produtividade durante o enchimento de grãos. Resultados efetivos também foram obtidos ao combinar todos os estágios. A análise com VANT mostrou-se uma alternativa promissora, eliminando a limitação de cobertura de nuvens de satélites, oferecendo alta precisão cartográfica, registros históricos em áreas extensas e menor tempo operacional em comparação a sensores ópticos de campo e métodos tradicionais.

Palavras - Chave: Veículo Aéreo Não Tripulado (VANT); eficiência de utilização de nutrientes; índices de vegetação; arroz

INTRODUCTION

Fertilizers are essential for the full development of agricultural crops, especially nitrogen (N), one of the nutrients that most limit plant growth (Ali et al., 2025). Deficient N availability results in yellowish leaves and reduced growth, while excess leads to darkened foliage and compromised yield. When applied above the plant's absorption capacity, nitrogen becomes a pollutant, with losses occurring through volatilization, immobilization by microorganisms, and leaching. Insufficient nitrogen availability can significantly restrict plant growth and development, whereas adequate supply stimulates root growth by increasing root volume, area, diameter, and total and primary root length, as well as root dry mass (Wang et al., 2024), ultimately enhancing nutrient uptake, improving nutrient balance, and boosting overall biomass production. Therefore, efficient nitrogen management is one of the most important practices to ensure the sustainability of agricultural production systems, impacting both economic viability and environmental quality. The quantification and determination of the optimal time to apply N doses is performed based on the nutritional status of the plants, which is particularly relevant for lowland rice, as nitrogen deficiency is one of the most important nutritional disorders in these production systems worldwide, directly influencing fertilizer recommendations and management strategies (Fageria & Baligar, 2001 Wu et al., 2024). Therefore, commonly, chemical analyses of plants are conducted through destructive sampling, known as direct determinations of plant tissue. This traditional method requires extensive fieldwork and subsequent laboratory analysis, and even so, with this great human effort, the sample size is usually limited, as it is a spatial representation based on points; in addition, the collection and analysis phases take an important time and the association of the state of the plants may not be perfectly associated with other factors present in the field. An alternative method is indirect estimates, which may be based on capturing the radiation reflected by the plant canopy, and the incident radiation to determine the reflectance. In this method, based on remote sensors, reflectance is measured in wavelengths along the electromagnetic spectrum, and the use of visible and near infrared bands is recurrent, with which it is possible to calculate numerous vegetation indices used to determine vegetation parameters (Gupta & Pandey 2021)

Specifically in this method, remote sensing is used in the monitoring of leaf nitrogen, due to the chlorophyll content positively correlated with the N content in the plant (Xu et al., 2023). Vegetation indices can discriminate different chlorophyll contents and biomass accumulation, with consequent recognition of plants better nourished with N (Narmilan et al., 2022). The information is acquired by ground, aerial, and orbital sensors, without physical contact with the studied object. Ground sensors are commonly referred to as proximal, due to their nature of operating close to the target and can be used manually or mounted on agricultural machinery. An example of this type of sensor are spectroradiometers, which capture detailed spectral information, without generating images and with point collections, while orbital and aerial remote sensing covers extensive areas of land, generating digital images. An additional advantage of orbital and aerial sensors refers to the ability to detect variability within the agricultural field, with results in images that facilitate decision-making by the analyst/farmer.

The use of remote sensing in this field of knowledge has been consolidated for some years and remains widely applied today, particularly in correlating nitrogen content with vegetation indices (Han et al., 2001; Jiang et al., 2025). Much of the literature highlights the use of proximal sensors across different agricultural crops (Lu et al., 2025), as these devices enable detailed assessments at the plant or plot scale. However, at the orbital level, nitrogen estimates from satellite imagery remain relatively scarce (Segarra et al., 2023). This is partly due to the need for model calibration through extensive and costly field campaigns, combined with inherent limitations such as low revisit frequency and coarse spatial resolution, despite the advantage of large-area coverage.

More recently, the use of unmanned aerial vehicles (UAVs) for remote sensing applications aimed at discriminating nitrogen content in plants has grown significantly, although its integration into agricultural research is still relatively recent. While proximal sensors remain valuable, their point-scale operation and low efficiency limit scalability. In contrast, UAVs equipped with multispectral, RGB digital, or thermal infrared sensors can deliver high-resolution, scalable spectral data over extensive agricultural areas (Bouguettaya et al., 2022). Recent studies illustrate this potential. For example, Li et al. (2024) used UAV-based RGB imagery to extract vegetation indices and texture features, enabling the estimation of nitrogen concentration in cotton leaves. In another approach, Peng et al. (2024) combined vegetation indices derived from UAV hyperspectral imagery with deep learning models to predict leaf nitrogen content (LNC). Complementing these efforts, Carracelas et al. (2025) applied UAV multispectral imagery to monitor nitrogen uptake in rice fields, aiming to evaluate irrigation efficiency. Collectively, these findings indicate that UAV-derived spectral datasets can effectively support the assessment of crop nitrogen status, including biomass, yield, chlorophyll content and nitrogen concentration, under diverse conditions. Nevertheless, a considerable knowledge gap remains regarding the accuracy, robustness and applicability of these technologies across different crops and environmental contexts.

Thus, the objectives of this study are: (1) to compare the effectiveness of the images obtained by UAV and the data from the proximal sensor (Crop Circle) in relation to the field data to estimate the leaf area index (LAI) and the nitrogen content in the plant (LNC) of the rice; (2) to determine the phenological phases of the wetted rice crop with such technologies, based on the estimation of the agronomic parameters above-ground biomass (AGB), LAI, LNC and crop productivity.

MATERIALS AND METHODS

Study area

The study area is located between the geographical coordinates latitude 16° 26’ 14” (S), longitude 49° 23’ 50” (W) and altitude of 720 m, located at the Embrapa Rice and Beans experimental station, at Fazenda Palmital, municipality of Goianira, Goiás, Central-West region of Brazil (Figure 1). The location has an Aw climate classification, which is Tropical Wet, with an average annual temperature of 19.3C and average annual rainfall of 1,600 mm (FAO, 1985). The soil of the region is classified as haplic Gleysol.

The experiment was conducted in the 2020/2021 harvest. The research design occurred in randomized blocks (DBC) with four replications in a split-plot scheme. In the main plot are the rice cultivars BRS Catiana and IRGA, followed by the subplots with varying doses of N in coverage (0, 50, 180 kg of N, in the form of urea). The planting date was 11/09/2020 and the harvest on four dates (March 1, 11, 18 and 25, 2021, depending on the cultivar and the dose of N). The base fertilization was 280 kg/ha N-P-K, with formulation 5-30-15, respectively. At planting, 80 seeds were placed per linear meter, with plant spacing of 0.17 m.

Fig. 1. Location of the study area in the municipality of Goianira, Goiás, Brazil (left) and aerial image "Red Green Blue" (RGB) of the experimental plots with different N rates.

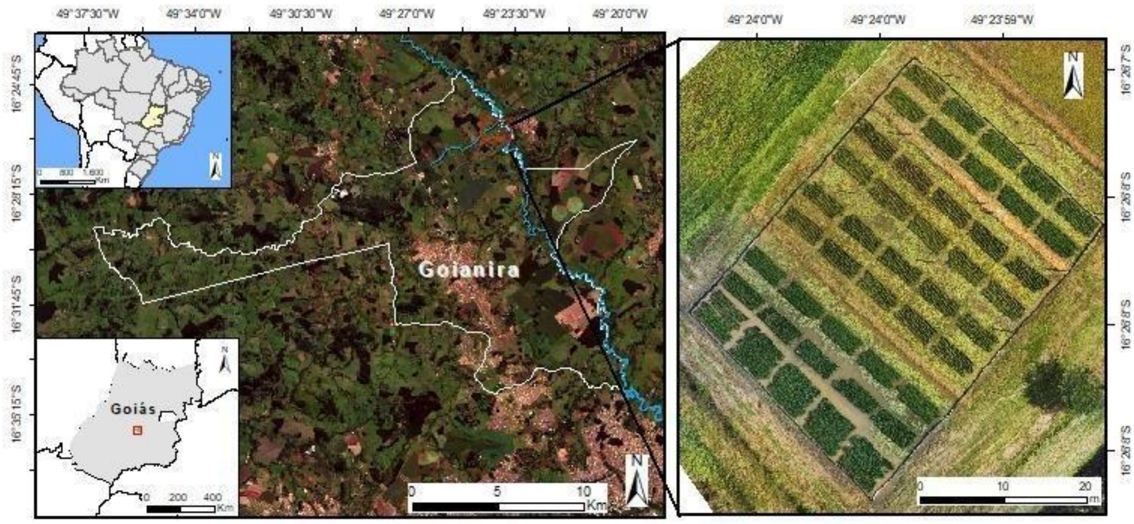

Data collection

The set of data obtained with the experiment originated in three different forms of collections. The first consisted of obtaining the agronomic parameters above-ground biomass (AGB), leaf nitrogen content (LNC), leaf area index (LAI) and rice productivity, referred to here as field data (DC), obtained through destructive samples. The second phase refers to the imaging using a UAV (Parrot - Bluegrass), embedded with a multispectral camera (Parrot - Sequoia), from which the reflectance orthomosaics of the Red, Green, Red Edge and NIR bands were obtained. The third phase took place through the proximal sensor, with which the NDVI and NDRE indices of the rice canopy were obtained.

The rice cycle was divided into four periods, in which the samples were grouped. The relationship of available samples to DC and UAV are reported in Table 1. As the DCs were obtained by destructive samples, the amount of data collected in each evaluation was variable, being higher in the last collection in which the plants were collected just before physiological maturation. The relationship of available data with DC and indices from the proximal sensor is also presented in Table 1.

Table 1. Relation of the number of samples by variables collected in the field, associated with the reflectance data obtained by imaging with a multispectral sensor embedded in a UAV and the vegetation index data obtained with a *Proximal Sensor* (SP), with the samples grouped by phenological stage. Field data collection and nitrogen status parameters.

Phenological Stage	DAE	Dry Biomass		LAI		Nitrogen	
		UAV	SP	UAV	SP	UAV	SP
Vegetative	16	-	8	-	23	-	7
Vegetative	30	16	16	24	24	24	24
Reproductive onset	47	-	-	24	24	21	21
Reproductive onset	54	24	24	24	24	24	24
Reproductive	69	-	-	24	24	24	24
Reproductive	79	24	24	24	24	24	24
Grain filling	97	40	19	39	19	40	19

The N status of rice was evaluated by the agronomic parameters AGB, LNC and LAI, obtained in the analysis of rice plant samples, systematically collected at different positions within each plot, where twenty plants were randomly sampled and the average value of each parameter was assigned to the experimental unit. The samples were divided into 50% fresh plants (leaf and stem) that were dried in a forced ventilation oven at 75°C to a constant mass, to obtain AGB, and 50% fresh plants to determine LNC using the methodology of Tedesco et al. (1995). The leaf area index (LAI) (Equation 1) was calculated from the leaf area (LA inm) obtained with the LI-3100 photoelectric area meter (Li - Color. Inc. Lincoln, Nebraska, USA).

$$LAI= LASA \qquad (1)$$

Where, LA is the sampled leaf area; SA is the soil area corresponding to the collected LA sample.

Grain yield was determined at physiological maturity for each plot. All plants within the central rows of a 1 m² area were harvested at ground level to avoid border effects. The panicles were threshed, and the grains were weighed after drying to a standard moisture content of 13%.

Productivity was expressed as kilograms per hectare (kg ha^{-1}). For treatments with different harvest dates, yield was determined separately for each plot according to its maturity stage.
The proximal optical sensor used was the Crop Circle ACS-430 (Holland Scientific Inc., Lincoln, NE, USA). This is based on a polychromatic light source that registers three spectral bands: 670 ± 11 nm (red, R), 730 ± 10 nm (RE) and >760 nm (NIR), with a collection frequency of 10 Hz per second. With this sensor, collections were made 1 meter above the rice crop canopy, for comparison with UAV data, selecting the most widely used vegetation indices (IVs, Table 2).

UAV Data

The imaging sensor used was the Parrot - Sequoia camera aboard the Bluegrass UAV, a quadcopter rotary wing. The camera records four-band multispectral images, with 1.2 MP spatial resolution, in the range of green (550 nm +/- 40 nm), red (660 nm +/- 40 nm), red edge (735 nm +/- 10 nm) and near infrared (790 nm +/- 40 nm), in addition to an RGB camera (16 MP, 4608 × 3456 pixels). Reflectance was calibrated by two methods: in the first, before each flight, photos of a reflectance calibration panel (positioned on the ground, without shadow) were captured, later used as standards to calibrate each of the bands; in the second method, a sensor integrated into the upper plane of the UAV captured and recorded the light conditions at the time of capture of each image, so that the reflectance adjustment is performed during processing, using the sensor records.

Imaging always took place between 10am and 12pm to avoid shading inside the canopy. The flight height was 30 meters, resulting in a GSD of 3.5 cm/pixel for the orthomosaics of the spectral bands. The overlap between the photos was 70% frontal and 70% lateral. The flight plan and image acquisition were performed by the Pix4D Capture application (version 4.2.27) (for *mobile* equipment). Images of the reference calibration panel were collected with nadir view before each flight. At the time of post-processing these images were used to calibrate the multispectral data. Pix4D Mapper software (Pix4D, Prilly, Switzerland) was used to process the images in order to generate the Digital Surface Model and the orthomosaic - in georeferenced reflectance scale, for each flight.

A total of seven orthomosaics (in reflectance) for each of the four spectral bands were obtained throughout the culture cycle, making it possible to calculate several IVs. In this study, those with a history of use for biomass and nitrogen prediction were selected (Table 2). The limits of each agricultural plot were elaborated and used as a region of interest to calculate the average of the pixels of the IVs, in order to relate them to the AGB, LAI and LNC OBTAINED on the surface. Within the regions of interest, any fractions corresponding to exposed soil were discarded; this procedure was done through a canopy classification threshold with the EVI2 index.

In each plot, the average value of each IV was extracted within the highlighted region, using the zonal statistics tool of ArcGis Desktop software (version 10.8). The records were exported to a CSV spreadsheet and later used for data analysis.

Table 2. List of IVs calculated with UAV and proximal sensor.

Vegetation Index	Abbreviation	Formula	Reference
Canopy Chlorophyll Content Index	CCCI	(NDRE)/(NDVI)	Long et al. (2009)
Green Chlorophyll Index	CI green	(NIR / GREEN) -1	Gitelson et al. (2005)
Chlorophyll Vegetation Index	CVI	NIR * RED/GREEN2	Vincini et al. (2008)
Improved Vegetation Index 2	EVI2	2.5 (NIR - RED) / (NIR+ 2.4 * RED + 1)	Jiang et al. (2008)
Vegetation index difference normalized to green	GNDVI	NIR - GREEN) / (NIR + GREEN)	Gitelson et al. (1996)
Modified Chlorophyll Absorption in the Reflectance Index	MCARI	(REG - RED) - 0.2 (REG - GREEN) (REG / RED)	Daughtry et al. (2000)
Modified Photochemical Reflectance Index	MPRI	GREEN - RED / GREEN + RED	Yang et al. (2008)
Vegetation Index Adjusted by Modified Soil	MSAVI	(2 NIR + 1 - sqrt ((2 NIR + 1) 2 - 8 (NIR - RED))) / 2	Qi et al. (1994).
Meris terrestrial chlorophyll index	MTCI	(NIR - REG)/(REG - RED)	Dash et al. (2004)
Vegetation Index Modified Triangular 2	MTVI2	1.5(1.2(NIR-GREEN) - 2.5(RED-GREEN))√((2NIR+1)²-(6NIR-5√(RED))-0.5)]	Habouance et al. (2002)

Normalized Difference Red Edge	NDRE*	(NIR−REG) /(NIR+REG)	Fitzgerald et al. (2006)
Normalized Difference Vegetation Index	NDVI*	(NIR - RED) / (NIR + RED)	Rouse et al. (1974).
Normalized Difference RedEdge/Red	NDVIre	(REG-RED) / (REG+RED)	Gitelson & Merzlyak, (1994)
Optimized Soil-Adjusted Vegetation Index	OSAVI	1.16 (NIR - RED) / (NIR + RED + 0.16)	Rondeaux et al. (1996)
Relative Vigor Index	RVI	NIR/RED	Pearson and Miller (1972)
Soil-Adjusted Vegetation Index	SAVI	(1 + L) (NIR - RED) / L + NIR + RED	Huete (1988).
Triangular Vegetation Index	TVI	0.5 (120 (NIR - GREEN) - 200 (RED - GREEN))	Broge et al. (2001).

* Vegetation indices calculated for the Crop Circle ACS-430 proximal sensor.

Statistical data analysis

First, the proximal sensor and the multispectral camera (on board the UAV) were compared to estimate LNC and LAI using the NDVI and NDRE indices. Initially, the correlation between proximal sensor and UAV was assessed by Pearson's method. In sequence, linear models were adjusted between agronomic parameters and vegetation indices, for each cultivar and phenological stage, and for the phenological stages with the grouped cultivars. The data were divided into two subsets, one for training and one for testing, in the proportion of 60% and 40%, respectively. The performance of the models was evaluated using the coefficient of determination (R^2) (Equation 2), absolute mean error (MAE) (Equation 3) and square root of the mean square error (RMSE) (Equation 4), available in the caret package developed for R language (Kuhn, 2008).

Next, the fit of empirical models of multiple linear regression was evaluated for estimating agronomic parameters using vegetation indices obtained by remote sensing with UAV as predictors. Initially, the association between the parameters and IVs was explored through Pearson's correlation, elaborating a correlation matrix for each collection, in order to verify the occurrence of collinearity between IVs and which would be predominantly associated with agronomic parameters. For model adjustments, the *stepwise* regression method was used, using the SignifReg package implemented in R (Zambom & Kim, 2022).

The selection criteria were the highest values of R², p-value of input and output at < 0,05, adjusted by the *FDR* (False Discovery Rate) method, which calculates the ratio between false positive results and positive results, reducing the chances of the true hypothesis being rejected. *Stepwise* regression works in a step-by-step interactive way, adding (*forward*) or removing (*backward)* variables from the selection of variables that have a significant contribution to the model. After adjusting the model, the assumptions of normality and homoscedasticity were verified using the Dharma packages (Hartig, 2022).

Model performances were also evaluated by R², MAE and RMSE, calculated by the *k-fold* cross-validation method in five resampling interactions. In this method, the data set is divided into *k* subset, then the model is trained with *k-1* subsets of the data and validated with the remainder; this process occurs in a *loop*, *k* times. The performance measures (R², MAE and RMSE) of the model correspond to the average of the values calculated in each interaction or *loop*. This method allows the data to not be wasted by allocating it only for testing, or for the test data to be arbitrarily selected, allowing the model to be trained and assessed with the widest distribution of values.

$$R^2 = \left[1 - \frac{\sum_{i=0}^{N-1} (y-\hat{y})^2}{\sum_{i=0}^{N-1} (y-\hat{y})^2}\right] \quad (2)$$

Where N is the number of observations; ŷi is the i-th model prediction; yi is the i-th observation; and ȳ is the mean of the observations.

$$MAE = \frac{\sum_{i=1}^{n} \left|E_i - O_i\right|}{N} \quad (3)$$

Where, Oi is the current value; Ei is the estimated value; N is the number of observations.

$$RMSE = \sqrt{\frac{\sum_{t=0}^{N-1} \left(y-\hat{y}\right)^2}{N}} \quad (4)$$

Where N is the number of observations; ŷi is the i-th model prediction; yi is the i-th observation; and ȳ is the mean of the observations.

For data analysis, the statistical program R (R Core Team) was used.

RESULTS AND DISCUSSION

Comparison between UAV and proximal sensor for LNC and LAI estimation

The correlation between sensor readings for NDVI and NDRE vegetation indices is low (Table 3); this suggests a possible divergence in sampling or resolution. During sampling, the proximal sensor reads the center lines on the canopy and the average value is computed for the plot, making it possible to obtain the reading curves and disregard discrepant values that could not correspond to the vegetation. However, this is based on values only. On the other hand, the reflectance orthomosaic obtained by the UAV allows the researcher to define the sample area, considering beyond the central lines and disregarding only the border region, which suffers more from the effects of adjacent plots. In addition, it is possible to base the selection not only on values, but also on features, such as rice plants, avoiding that values obtained from the canopy are disregarded only because they are considered discrepant.

Table 3. Matrix with Pearson correlation between NDVI and NDRE vegetation indices obtained with crop circle sensor and UAV-embedded multispectral camera.

	NDVI-Crop Circle	NDRE- Crop Circle	NDRE-UAV	NDVI-UAV
NDVI- Crop Circle	1	-	-	-
NDRE- Crop Circle	0.99	1	-	-
NDRE-UAV	0.35	0.34	1	-
NDVI-UAV	0.23	0.22	0.74	1

In the vegetative stage, IVs derived from UAV did not present a linear trend, both for joint analysis and for separate cultivars (Table 4). The data obtained by the proximal sensor in the vegetative stage showed a linear trend (R = 0,89 and 0,85 for NDRE and NDVI, respectively), but with low accuracy (RMSE = 6,41 and 4,92; MAE = 5,66 and 4,17 for NDRE and NDVI, respectively). This suggests that the canopy in the analyzed period was affected by the presence of bottom represented by water and soil. As reported by Molin et al. (2010), the low demand for N by the crop in the early stages did not cause significant changes in NDVI to predict LNC. Additionally, the low correlation with the IV may be related to the considerable influence of soil/water layer, due to reduced biomass.

In the grain filling stage, IVs were inefficient in estimating LNC, suggesting that NDVI and NDRE saturated from the reproductive stage (Brinkhoff et al., 2019). In situations where NDVI is high, its ability to detect changes in biomass becomes less sensitive, which is commonly referred to as an asymptotic saturation phenomenon (Risso et al., 2012). Gnyp et al. (2014) report that selecting near wavelengths that are able to effectively penetrate the plant canopy, and combining this information appropriately, can help reduce saturation and improve the accuracy of plant-related measurements or evaluations. Thus, in the treatment of the data based on the multispectral sensor on board the UAV, the combination of all bands was investigated through several IVs.

The best performing model to estimate LNC was the NDVI using UAV data in the analysis of the two rice cultivars together, at the stage of reproductive initiation (R= 0,92). The model based on the proximal sensor showed a high linear relationship with the NDRE, but with low precision (R = 0,89), from the vegetative stage to the IRGA cultivar, with a decrease throughout the development of the rice crop. Based on the selection criteria, the best fit model for the proximal sensor was with the NDRE for the two cultivars at the beginning of the reproductive stage (R = 0,84).

To estimate the LAI (Table 5), the joint analysis of the two cultivars also showed a superior result, both with the use of NDRE (R = 0,88) and NDVI (R = 0,86), for UAV-based estimates. The proximal sensor most effectively estimated the LAI from the separately analyzed cultivars. The best model was for the Irga cultivar, in the early reproductive period, with NDVI (R = 0,85). When the results for the two cultivars were observed, the correlation coefficients were lower with a moderate coefficient of determination. In general, as the LAI increases, vegetation indices are expected to increase as well, as there will be more foliage to reflect light in the spectral region captured by the sensor. This is because a greater number of leaves tends to result in a greater absorption of light in the visible range and a lower reflection in the near-infrared range, which is reflected in the values of vegetation indices (Manes et al., 2001). However, the relationship between LAI and vegetation indices may not be linear in all situations, especially in areas with different types of vegetation cover, plant phenological stages and environmental conditions. In addition, other factors, such as foliage structure, soil moisture and the presence of non-green vegetation, can also influence this relationship (Xu et al., 2020). In our study, in the final periods of the cycle, where there is a greater amount of foliage (greater LAI), there is also the presence of grains that modify the values of the IVs, usually lowering the average of these. Thus, lower performance of the models in the grain filling stage is observed.

Table 4. Regression analysis to estimate leaf nitrogen content (LNC) based on UAV and proximal sensor (Crop circle) data.

Cultivar	Phenological Stage	NDRE – Proximal sensor				NDRE - UAV			
		RMSE	MAE	R^2	Equation	RMSE	MAE	R^2	Equation
Catiana	Vegetative	3.00	2.10	0.44	35.366 - 8.906x	4.54	3.88	0.00	8.919 + 129.49x
	Reproductive onset	1.73	1.32	0.65	-2.054 + 20.263x	1.24	1.23	0.78	6.194 + 42.828x
	Reproductive	4.37	4.11	0.33	-22.207 + 40.241x	1.21	1.07	0.53	-1.052 + 53.281x
	Grain filling	3.02	2.38	0.00	-17.687 + 33.91x	2.94	2.13	0.14	0.363 + 67.873x
Irga	Vegetative	6.41	5.66	0.89	35.366 - 8.906x	8.24	7.09	0.00	8.919 + 129.49x
	Reproductive onset	3.40	3.29	0.25	-2.054 + 20.263x	2.46	2.44	0.65	6.194 + 42.828x
	Reproductive	4.05	3.23	0.32	-22.207 + 40.241x	2.30	2.04	0.85	-1.052 + 53.281x
	Grain filling	0.64	0.64	-	-17.687 + 33.91x	2.53	2.53	-	0.363 + 67.873x
Two cultivars	Vegetative	5.58	4.77	0.00	-18.76 + 35.751x	4.66	3.77	0.55	3.004 + 56.35x
	Reproductive onset	1.53	1.24	0.84	1.498 + 16.101x	1.35	0.80	0.85	6.817 + 40.743x
	Reproductive	3.90	3.45	0.64	-5.017 + 18.761x	3.50	2.79	0.86	2.622 + 34.936x
	Grain filling	2.94	2.41	0.35	-0.476 + 29.027x	1.77	1.34	0.63	22.276 + 29.874x

		NDVI – Proximal sensor				NDVI - UAV			
Catiana	Vegetative	2.74	1.89	0.30	15.278 + 12.357x	4.26	3.67	0.01	13.074 + 24.379x
	Reproductive onset	1.55	1.39	0.64	-0.327 + 18.43x	0.94	0.93	0.88	1.586 + 18.01x
	Reproductive	3.34	3.14	0.32	-13.816 + 29.59x	1.99	1.87	0.04	-18.994 + 38.564x
	Grain filling	2.99	2.22	0.01	-16.346 + 31.956x	2.67	2.55	0.17	4.741 + 12.242x
Irga	Vegetative	4.92	4.17	0.85	15.278 + 12.357x	6.34	5.33	0.07	13.074 + 24.379x
	Reproductive onset	3.53	3.38	0.18	-0.327 + 18.43x	3.02	2.95	0.50	1.586 + 18.01x
	Reproductive	3.33	2.47	0.26	-13.816 + 29.59x	2.47	2.34	0.60	-18.994 + 38.564x
	Grain filling	0.27	0.27	-	-16.346 + 31.956x	1.12	1.12	-	4.741 + 12.242x
Two cultivars	Vegetative	5.22	4.37	0.00	-16.346 + 31.956x	4.53	3.60	0.40	9.068 + 6.153x
	Reproductive onset	1.47	1.17	0.81	-0.327 + 18.43x	1.32	1.05	0.92	3.692 + 15.449x
	Reproductive	3.11	2.77	0.68	-13.816 + 29.59x	3.32	2.87	0.68	-11.38 + 28.309 x
	Grain filling	2.87	2.19	0.06	15.278 + 12.357x	2.45	1.96	0.48	20.632 + 10.243x

Table 5. Regression analysis for LAI estimation based on UAV and proximal sensor data (Crop circle).

Cultivar	Phenological Stage	NDRE – Proximal sensor				NDRE - UAV			
		RMSE	MAE	R²	Equation	RMSE	MAE	R²	Equation
Catiana	Vegetative	0.66	0.55	0.46	-2.411 + 5.33x	0.33	0.3	0.54	0.948 + 9.737x
	Reproductive onset	0.39	0.33	0.64	0.128 + 3.882x	0.52	0.44	0.26	1.905 + 7.164x

	Reproductive	1.59	1.56	0.24	-3.547 + 9.232x	0.57	0.48	0.06	0.8 + 14.296x
	Grain filling	0.58	0.49	0.14	-6.214 + 11.031x	0.61	0.54	0.01	0.841 + 15.891x
Irga	Vegetative	0.46	0.33	0.05	-2.411 + 5.33x	0.22	0.2	0.67	0.948 + 9.737x
	Reproductive onset	0.37	0.33	0.82	0.128 + 3.882x	0.47	0.46	0.48	1.905 + 7.164x
	Reproductive	0.58	0.56	0.58	-3.547 + 9.232x	0.74	0.66	0.57	0.8 + 14.296x
	Grain filling	0.98	0.98	-	-6.214 + 11.031x	0.17	0.17	-	0.841 + 15.891x
Two cultivars	Vegetative	0.52	0.47	0.43	1.743 + 0.779x	0.54	0.49	0.19	0.816 + 10.923x
	Reproductive onset	0.5	0.43	0.23	-0.474 + 4.597x	0.52	0.4	0.13	1.641 + 8.15x
	Reproductive	0.89	0.74	0.36	-4.358 + 9.829x	0.64	0.55	0.88	1.008 + 12.449x
	Grain filling	0.94	0.81	0.27	-9.671 + 14.906x	0.57	0.49	0.64	1.504 + 12.135x
		NDVI – Proximal sensor				**NDVI - UAV**			
Catiana	Vegetative	0.56	0.51	0.26	-0.708 + 3.392x	0.29	0.23	0.62	0.742 + 2.712x
	Reproductive onset	0.39	0.32	0.64	0.016 + 4.022x	0.56	0.48	0.17	1.104 + 3.015x
	Reproductive	1.25	1.21	0.35	-2.715 + 8.019x	0.5	0.42	0.18	-4.576 + 10.946x
	Grain filling	0.5	0.45	0.29	-6.13 + 10.658x	0.78	0.57	0.07	1.674 + 3.139x
Irga	Vegetative	0.41	0.29	0.05	-0.708 + 3.392x	0.21	0.18	0.7	0.742 + 2.712x
	Reproductive onset	0.33	0.29	0.85	0.016 + 4.022x	0.37	0.35	0.58	1.104 + 3.015x
	Reproductive	0.62	0.6	0.51	-2.715 + 8.019x	0.67	0.5	0.6	-4.576 + 10.946x

	Grain filling	0.58	0.58	-	-6.13 + 10.658x	0.48	0.48	-	1.674 + 3.139x
Two cultivars	Vegetative	0.43	0.38	0.44	-0.708 + 3.392x	0.55	0.48	0.2	0.617 + 3.062x
	Reproductive onset	0.47	0.39	0.25	0.016 + 4.022x	0.57	0.46	0.16	0.538 + 3.734x
	Reproductive	0.84	0.71	0.42	-2.715 + 8.019x	0.49	0.45	0.86	-3.992 + 10.101x
	Grain filling	0.89	0.72	0.01	-6.13 + 10.658x	0.86	0.63	0.29	3.643 + 0.148x

In this study, the proximal sensor was more suitable for measurements at the beginning of the reproductive stage, with a substantial drop in efficacy for subsequent stages. UAV showed higher performance in estimating agronomic parameters from the reproductive stage, with good performance in subsequent stages. When the accuracy of the UAV-based models, both for estimating LNC and LAI, is observed, they are substantially improved when the two cultivars are analyzed together. The proximal sensor presented difficulty in estimating agronomic parameters in certain stages, making the method more dependent on the reading time. In general, UAV-based models outperform those based on the proximal sensor in estimating LNC, as they present better performance and consistency of information throughout the cycle. Also, it is noteworthy that aerial surveying is faster and more practical to perform compared to the use of ground optical sensors, as in UAV, the sensor covers the entire area in less time, under the same illumination, allowing for a more optimized sampling of all agricultural plots in the field, besides providing aerial images suitable for other diagnostics and map elaboration.

The correlation between the actual and predicted values by the models, adjusted with the data grouped by cultivars, was good for the IVs obtained with UAV and proximal sensor. However, the indices obtained with UAV resulted in better agreement between the predicted and observed values; i.e., the data obtained with a proximal sensor resulted in models with a tendency to overestimate the LNC at low concentrations and underestimate it at high ones (Figure 2A). For all models, an incremental trend in residues was observed for the LNC; however, this effect is more pronounced in the models fitted with data obtained with the proximal sensor (Figure 2B).

Fig. 2. Performance of linear models with NDVI and NDRE, obtained by the proximal sensor (PS) Crop Circle and UAV-embedded multispectral camera, to predict the leaf nitrogen content of rice. A) Relationship between actual and predicted values by linear models. B) Residues of model estimates for actual values.

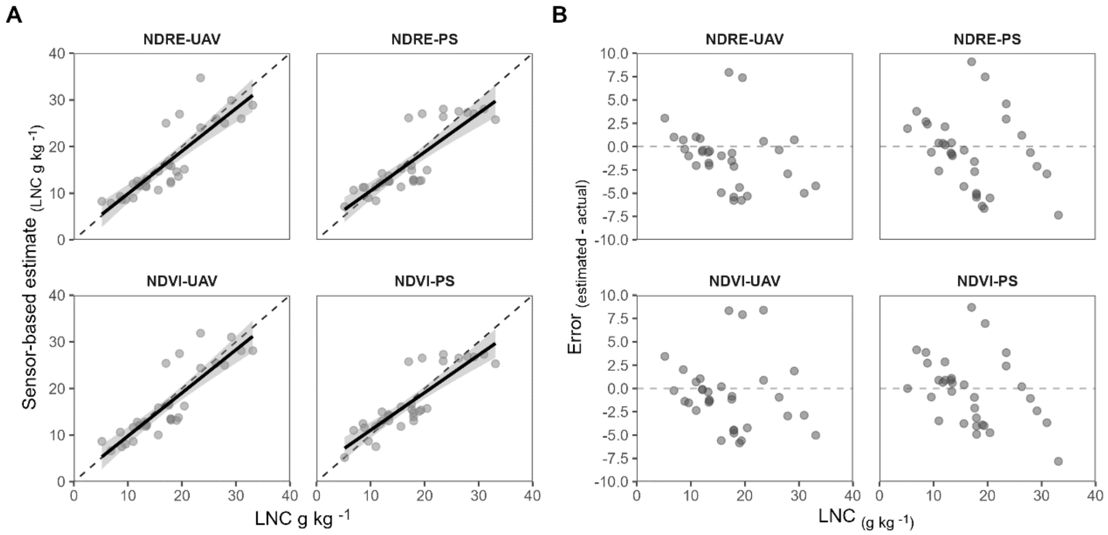

In general, the agreement between the estimated and actual LAI values was regular, however, among the values estimated downwards, LAI are slightly overestimated, while for high values, LAI are underestimated (Figure 3A). This effect is also notable in the residues, which present regular homogeneity of amplitude along the LAI; however, the amplitude of the residues of the prediction based on NDRE, coming from the proximal sensor, is notably greater. For NDVI, the same phenomenon is observed, although the dispersion is more discrete.

Fig. 3. Performance of linear models with NDVI and NDRE, obtained by the proximal sensor (PS) Crop Circle and UAV-embedded multispectral camera, for predicting the leaf area index (LAI) of rice. A) Relationship between actual and predicted values by linear models. B) Residues of model estimates for actual values.

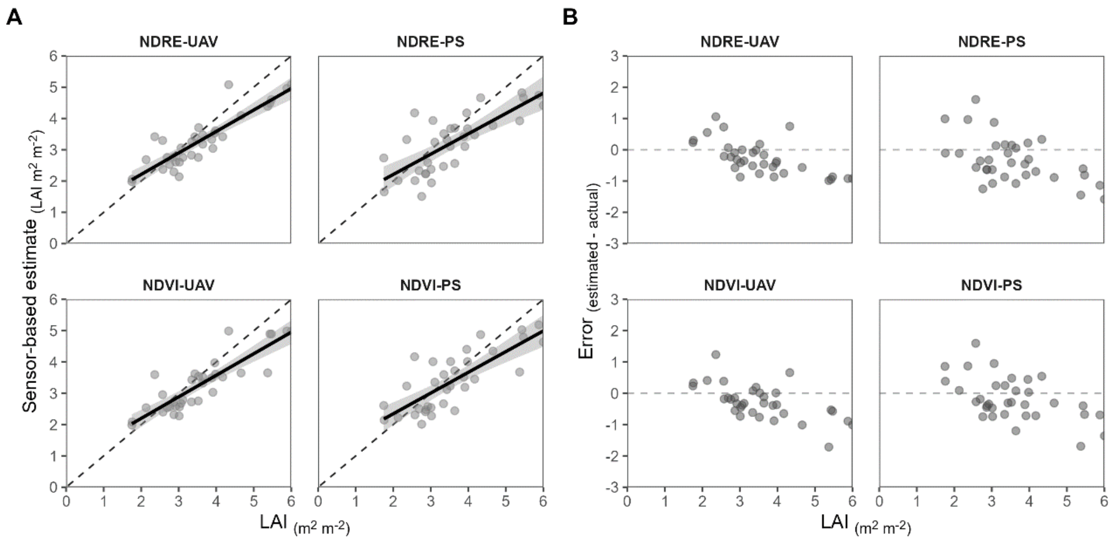

The linear models adjusted with the data of the grouped cultivars showed better performance when compared to those adjusted with the data of the cultivars separately. The coefficients of determination were higher, indicating that these two cultivars do not present a distinct covariance effect in the prediction of LNC and LAI. These results facilitate the application of the model, as it eliminates the need to separate plots between cultivars, being a simpler and more general model. Comparing the models based on indices of the same sensor and for the same cultivar cluster, it is possible to notice that the coefficients of the models were often different as a function of the phenological stages, suggesting a strong covariance effect, limiting the adjustment of a linear model based only on NDVI or NDRE to predict the parameters throughout the rice cycle.

Empirical models with vegetation indices for prediction of agronomic parameters in rice

Nitrogen Status Indicators

The data set obtained with the sampling conducted during the field evaluations showed a wide distribution (Table 6). This fact is important because the application of linear models for prediction is limited by the distribution of the data used for the fit. i.e., they usually perform well to estimate values within this distribution. The proximity between the median and mean values suggests a Gaussian distribution of the values, observed for the AGB, LAI and LNC PARAMETERS.

Table 6. Statistical summary of the parameters indicating nitrogen status in rice.

Parameter	n	min.	max.	median	q1	q3	iiq	dam	average	dp
AGB	112	1.09	163.72	40.36	19.34	69.842	50.502	40.453	49.853	37.504
LAI	182	0.97	6.76	3.275	2.4	3.94	1.54	1.245	3.291	1.292
LNC	164	5.19	36.89	12.21	9.125	17.581	8.456	5.589	14.607	7.368

Where, n: number of samples; min.: minimum value; max.: maximum value; q1: first quartile; q3: third quartile; iiq: interquartile range; dam: median absolute deviation; dp: standard deviation of the mean.

To initiate model fitting, selecting the IVs with the highest correlation with agronomic parameters would be a methodology; however, none of the IVs were highly correlated with agronomic parameters (Table 7). Because the coefficient of determination is the square of the correlation, only very high or perfect correlations would result in models with high coefficient of determination. Therefore, it is evident that using a single IV to predict nitrogen status parameters in rice throughout the rice cycle has its limitations and using the multiple linear regression method may be the most promising alternative. This considers adjusting the models for specific periods of the rice cycle. The method of selecting variables for *stepwise* regression allows the correlation analysis between the predicted and predictor variables to be in the background and the adjustment of the model to be done directly, considering as criteria the significance of the coefficients of the predictor variables and the coefficient of determination.

Table 7. Pearson Correlation between vegetation indices and nitrogen status parameters evaluated th roughout the rice cycle.

IV	LNC	AGB	LAI
CCCI	0.05	0.36	0.42
CLGREEN	-0.09	0.59	0.65
CVI	-0.09	0.44	0.41
EVI2	-0.19	0.62	0.65
GNDVI	-0.18	0.63	0.63
MCARI	0.09	-0.64	-0.72

MPRI	-0.16	0.48	0.62
MSAVI	-0.04	0.50	0.57
MTCI	-0.03	0.27	0.42
MTVI2	-0.03	0.45	0.50
NDRE	-0.02	0.41	0.55
NDVI	–0.21	0.61	0.63
NDVIRE	–0.21	0.58	0.62
OSAVI	-0.12	0.55	0.59
RVI	-0.08	0.59	0.70
SAVI	-0.08	0.52	0.57
TVI	-0.05	0.50	0.56

AGB - Above-Ground Biomass

In the models for the prediction of rice AGB in the reproductive phenological stages (Figure 4B) and grain filling (Figure 4C), the agreement between the predicted and observed values was strong, where the arrangement of the line indicates that the slope coefficient is close to 1. The errors (MAE and RMSE) in both models were numerically higher than those of the model adjusted for the beginning of the reproductive stage, with MAE at 0.25 and 0.28 and RMSE at 0.29 and 0.33 for the reproductive stages and grain filling, respectively. However, the errors correspond to the relatively small values with respect to the values of the dry biomass dataset (~0,6 to ~3,4) used to fit both models.

Estimates of AGB are recurrent in the literature, generally presenting good results with UAV data. Askari et al. (2019) obtained good accuracy in estimating biomass ($R \geq 0.77$) using models based on *stepwise* selection with field and UAV data in pasture areas. In the study by Niu et al. (2019), vegetation indices derived from UAV images had great potential to estimate the aerial biomass of corn, with Rvalues ranging from 0.63 to 0.73.

The model coefficients do not represent a causal relationship between the predictor variables and the predicted variable; this is common when the goal of regression is to interpret the effect of a given treatment on a variable where an increase or decrease is desired. In the case of this research, the predictor variables are dependent on the predicted variable, varying as a function of it and capturing its status. In this case, the collinearity between variables is not explored, while the same variables are not used as predictors throughout the crop cycle, since the objective is to obtain the best possible model for predicting dry biomass at each phenological stage.

Fig. 4. Performance of linear models with multiple predictors, obtained by a multispectral camera mounted on a UAV, for predicting leaf area index in rice. A) Relationship between actual and predicted values for the beginning of the reproductive stage. B) Relationship between actual and predicted values for the reproductive stage. C) Relationship between the actual and predicted values for the grain filling stage.

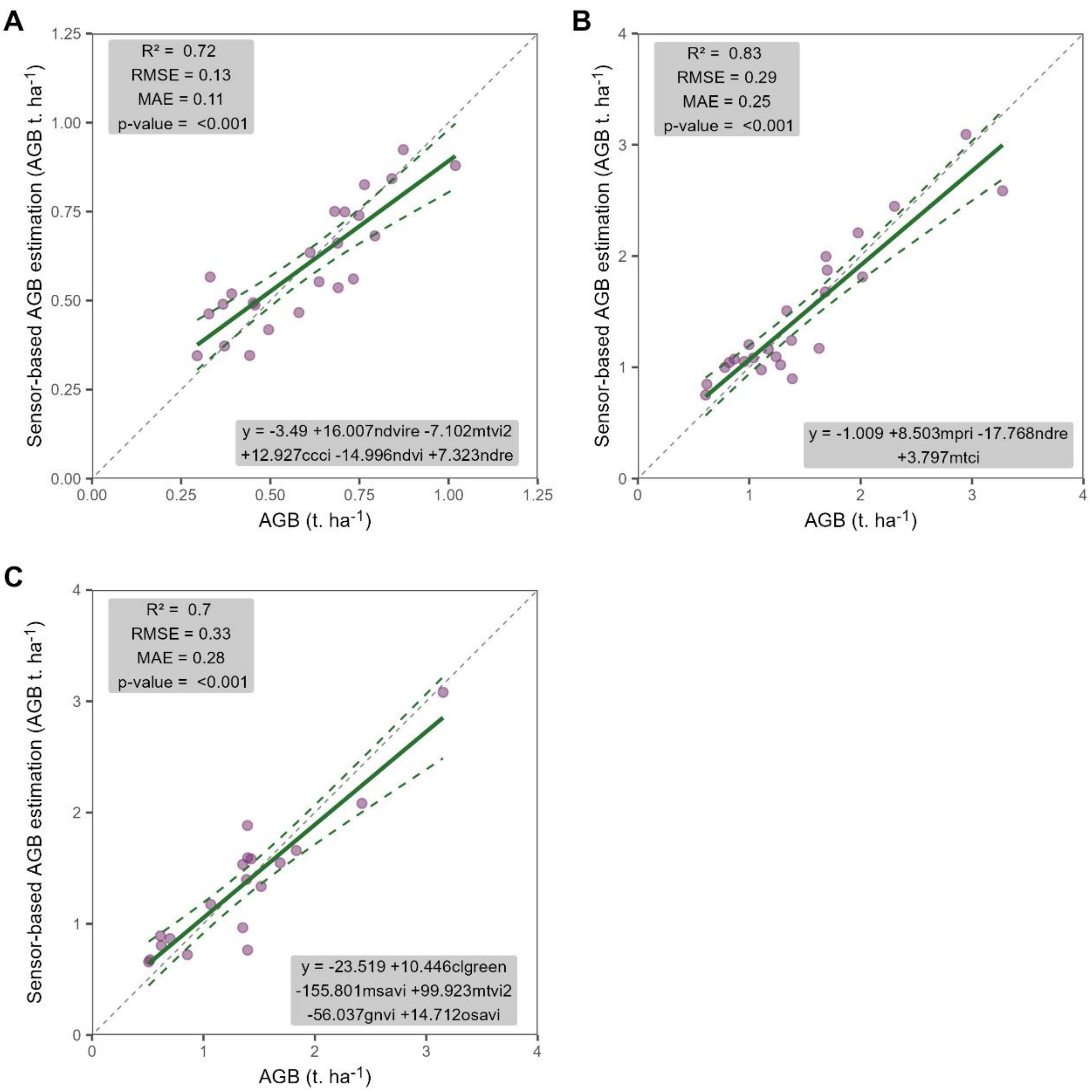

The model adjusted to estimate dry biomass throughout the rice cycle performed well, with high coefficient of determination and moderate errors, with close MAE and RMSE. The agreement between predicted and observed values is good, with a slight tendency to overestimate predicted values at low AGB concentration and underestimate at highs. But for intermediate values, the model shows a pattern of high agreement (Figure 5A). The residues present homogeneous dispersion between low and intermediate values, however, in higher values, there is a negative trend pattern, mostly referring to the AGB values of the grain filling stage (Figure 5B).

Fig. 5. Performance of linear models with multiple predictors, obtained by multispectral camera mounted on UAV for predicting above-ground dry biomass in rice. A) Relationship between actual and predicted values. B) Residues of model estimates for actual values.

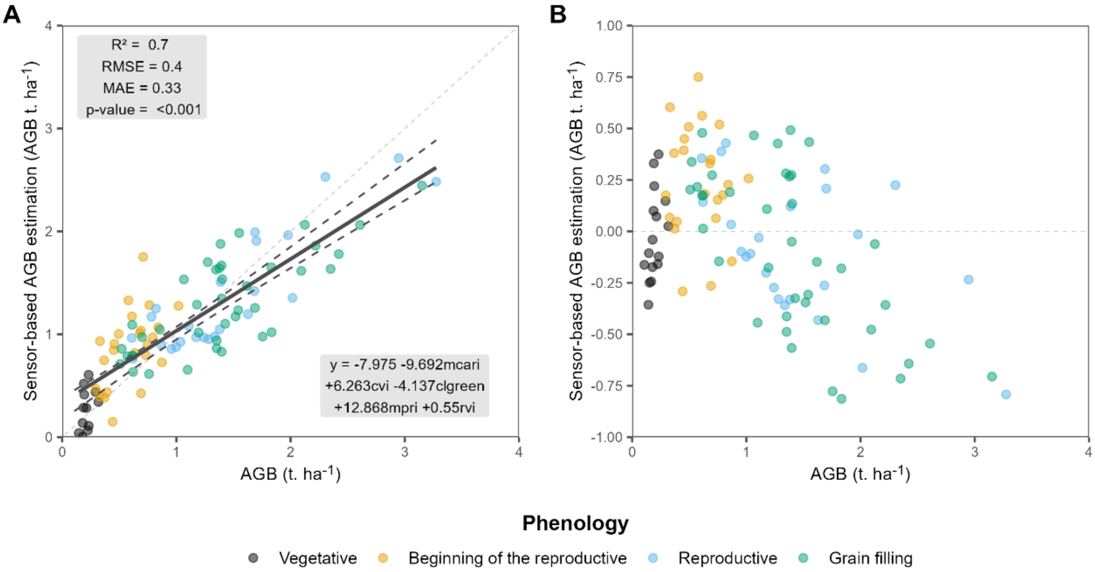

LAI- Leaf Area Index

The estimates of LAI in rice obtained by the linear multiple regression models are presented in Figure 6, in the vegetative (Figure 6A), early reproductive (Figure 6B) and grain filling (Figure 6D) phenological stages. The coefficients of determination were high (0,57 to 0,69), while the errors presented by the values of MAE (0.11 to 0.41) and RMSE (0.14 to 0.48) correspond to small fractions of the LAI values sampled in these stages. In the reproductive stage (Figure 6C), the coefficient of determination was very high, although the errors were numerically higher than those of the other models, and even though they correspond as the others to fractions of the LAI values sampled during this phenological stage. In the final stage analyzed (grain filling), the efficiency of the model reduced. Gong et al. (2021) also found better relationships in the middle of the rice cycle, in the reproductive stage (preheader), with saturation of the IVs analyzed in the post header.

Fig. 6 - Performance of linear models with multiple predictors, obtained by a multispectral camera mounted on a UAV, for predicting leaf area index in rice. A) Relationship between actual and predicted values for the beginning of the vegetative stage. B) Relationship between actual and predicted values for the beginning of the reproductive stage. C) Relationship between actual and predicted values for the reproductive stage. D) Relationship between the actual and predicted values for the grain filling stage.

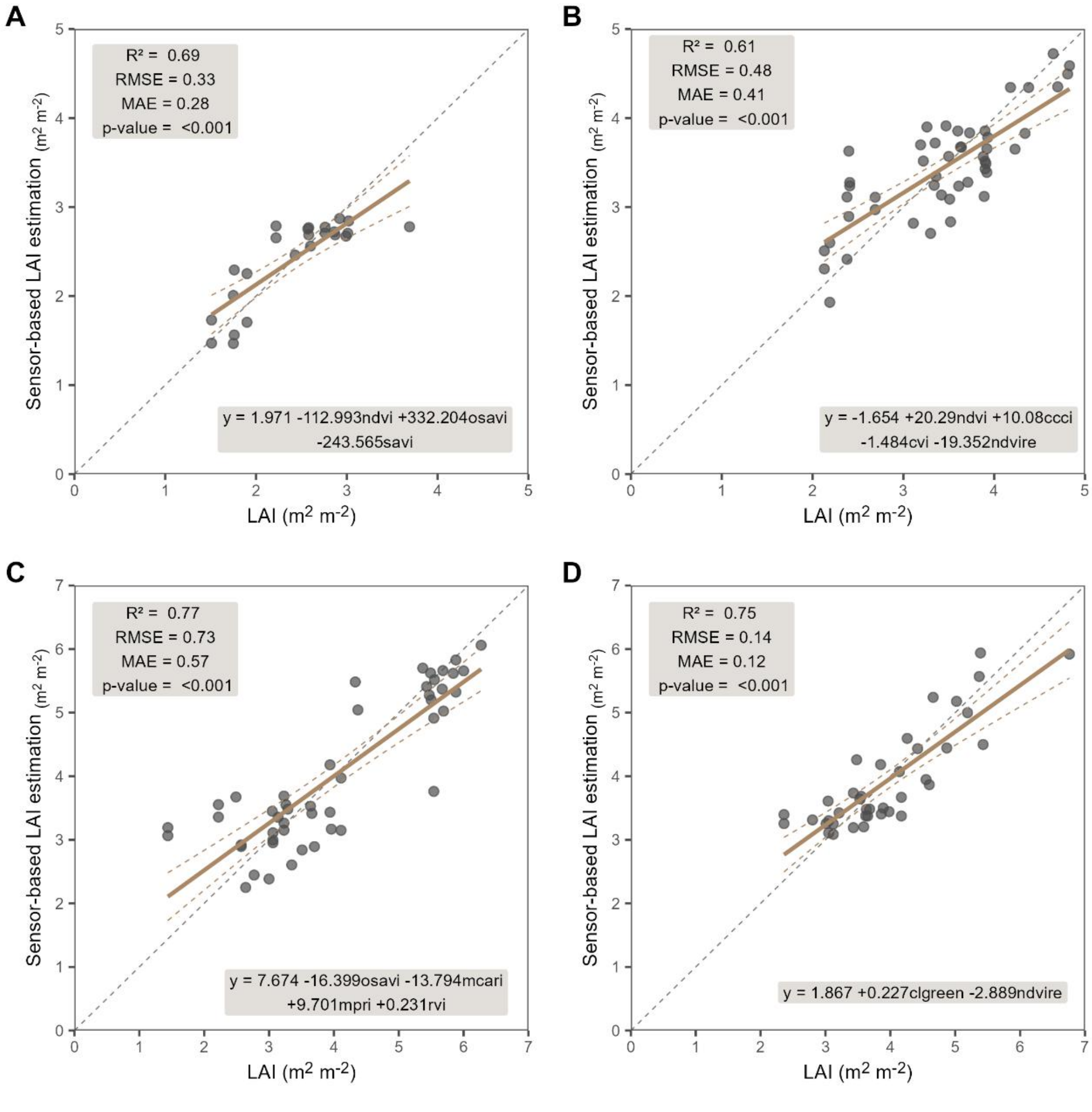

In addition to the models adjusted for each phenological stage, a model was adjusted for the entire rice crop cycle. This adjustment relied on six IVs and resulted in a coefficient of determination of 0.67. This is particularly interesting because the model contemplates the entire rice cycle. The errors estimated by MAE and RMSE were 0.52 and 0.64, respectively; they are relatively small values in the distribution of the sampled values. The agreement between actual and predicted values is strongly associated, with a slight tendency to overestimate LAI values at low indices and underestimate at high ones; however, this pattern is not associated with data from a phenological stage (Figure 7A). The residues present a slightly heterogeneous dispersion pattern, with a slightly positive trend in estimates of low LAI values and negative in high ones (Figure 7B). The model for predicting LAI in all rice stages presented similar performance to the models adjusted for specific stages, being plausible for a more pragmatic application.

Fig. 7 - Performance of linear models with multiple predictors, obtained by a multispectral camera mounted on a UAV, for predicting leaf area index in rice. A) Relationship between actual and predicted values. B) Residues of model estimates for actual values.

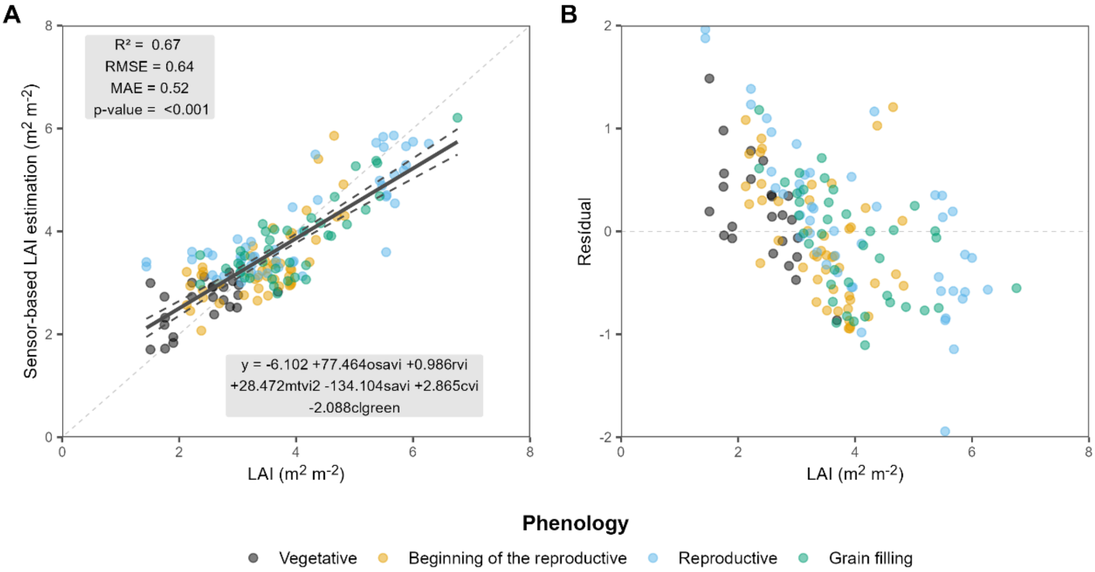

LNC- Leaf Nitrogen Content

Multiple regression between UAV-based IVs and LNC returned optimal and satisfactory results, with R ranging between 0.52 and 0.75, while the RMSE ranged between 1.61 and 3.52 (Figure 8). The best LNC prediction model WAS for the reproductive stage and used 3 indices formulated with the NIR, Red and Green bands. However, the coefficients of determination were high from the beginning of the reproductive, which indicates that the models proposed from this stage are suitable for estimating LNC. LNC prediction models, according to the stage of the crop, are essential for the efficient management of N in commercial crops (Fageria et al., 2003; Santos et al., 2021).

The agreement between predicted and actual values was strong in most models and nearly perfect in the model adjusted for grain filling stage (Figure 8D), with a discrete tendency to overestimate at low contents and underestimate at highs, most notable only at the vegetative stage (Figure 8A). Errors were low in all models, with the MAE and RMSE values remarkably close, indicating the absence of discrepant data with leverage power. All models showed a significant slope of the line, with most of them presenting a probability of significance lower than 0.001; only the model adjusted for the vegetative stage presented a higher probability, with a p-value of 0.0043, which still represents high significance.

Fig. 8 - Performance of linear models with multiple predictors, obtained by a multispectral camera mounted on a UAV, for predicting leaf area index in rice. A) Relationship between actual and predicted values for the beginning of the vegetative stage. B) Relationship between actual and predicted values for the beginning of the reproductive stage. C) Relationship between actual and predicted values for the reproductive stage. D) Relationship between the actual and predicted values for the grain filling stage.

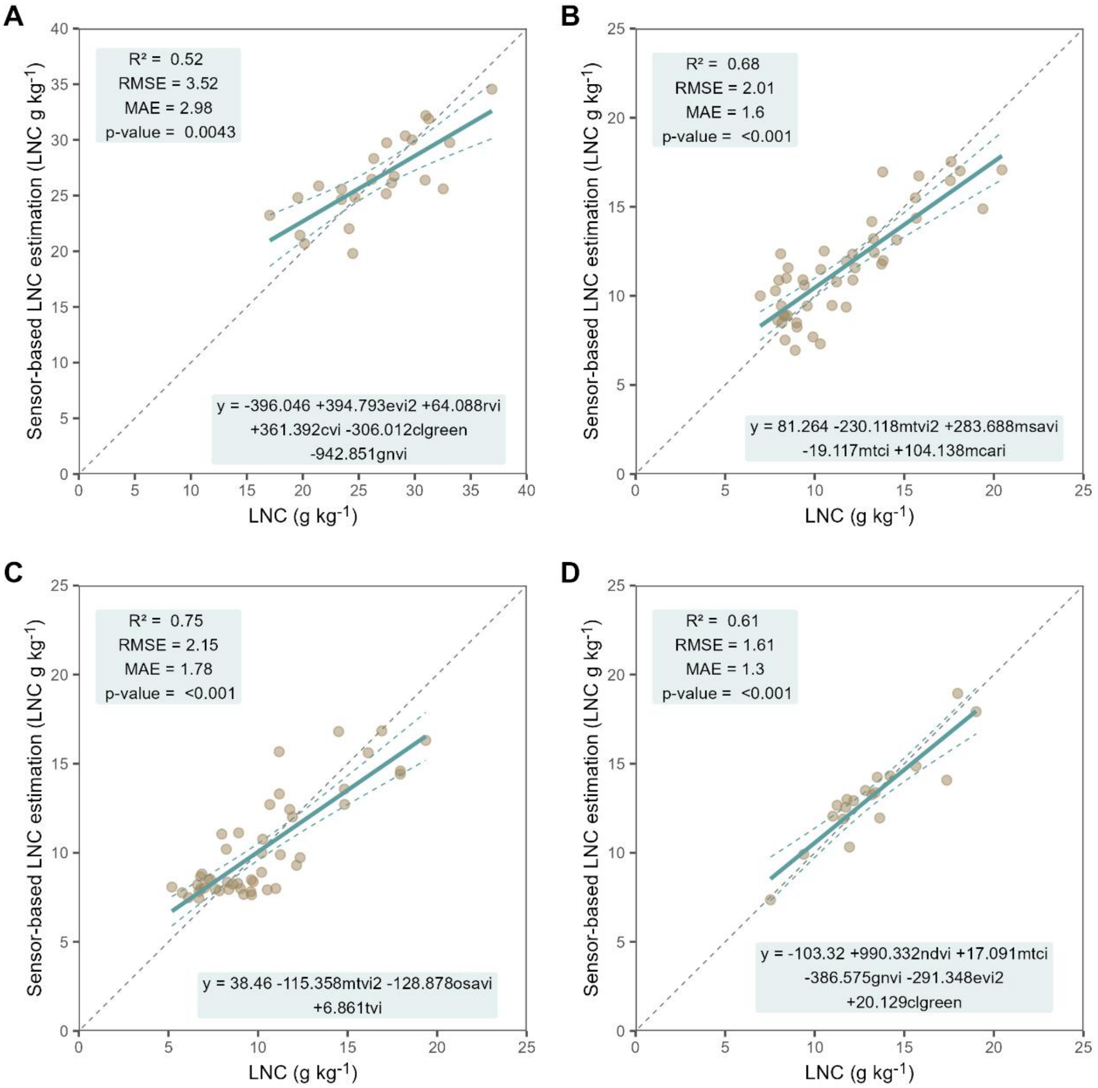

The model adjusted for prediction of LNC in vegetative phenological stages, beginning of reproductive, reproductive and grain filling in rice crop showed lower performance than those adjusted for each stage; the coefficient of determination was significantly lower, especially when compared to the model adjusted for the reproductive stage (Figure 8C). The error estimates represented by MAE and RMSE of this model were higher when compared to the stage models (Figure 8), with the most pronounced deviations for the predictions in the vegetative stage (Figure 9A). The model shows lower agreement when compared to the separate stage models, mainly influenced by the vegetative stage data that had a leverage effect. The residues present a regularly homogeneous dispersion, except for the vegetative stage, which presented mostly negative deviations (Figure 9B). Therefore, the model for predicting LNC throughout the rice cycle presented lower performance than the models adjusted for specific stages, and this approach was the most assertive.

Fig. 9 - Performance of linear models with multiple predictors, obtained by a multispectral camera mounted on a UAV, for predicting leaf area index in rice. A) Relationship between actual and predicted values. B) Residues of model estimates for actual values.

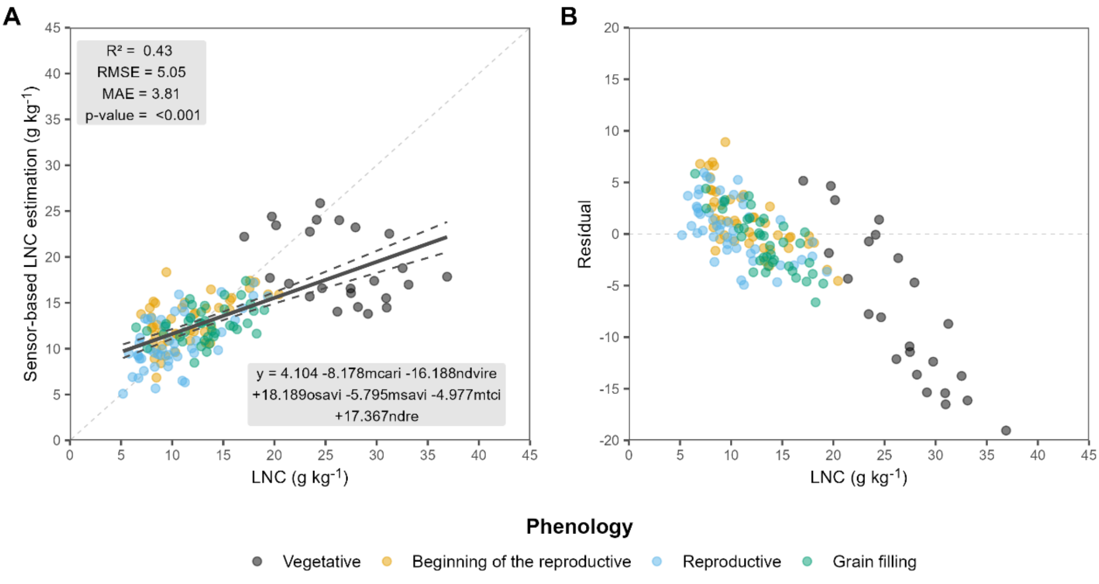

Empirical model with vegetation indices for rice yield estimation

Yield estimates enable harvest planning, processing, and commercialization, as well as revenue forecasting. Among the models for predicting productivity, the model adjusted with the data of the vegetation indices obtained in the grain filling stage showed the best performance

(Figure 10d). The model presented a remarkably high coefficient of determination, with a value of 0.83, and small errors, with MAE and RMSE values of 0.66 and 0.81, respectively.

The other models presented lower determination coefficients, larger errors and lower agreement, such as change of scale, overestimating in low productivity values and underestimating in high productivity values (Figures 10a to 10c). None of the models presented localization problems, an indication of high cartographic accuracy of the UAV. The error values reflect the accuracy of the model; in the case of the model based on the grain filling stage data, the errors were relatively small, with the MAE and RMSE values close.

Fig. 10 - Performance of linear models with multiple predictors, obtained by a multispectral camera mounted on a UAV, for predicting leaf area index in rice. A) Relationship between actual and predicted values for the beginning of the vegetative stage. B) Relationship between actual and predicted values for the beginning of the reproductive stage. C) Relationship between actual and predicted values for the reproductive stage. D) Relationship between the actual and predicted values for the grain filling stage.

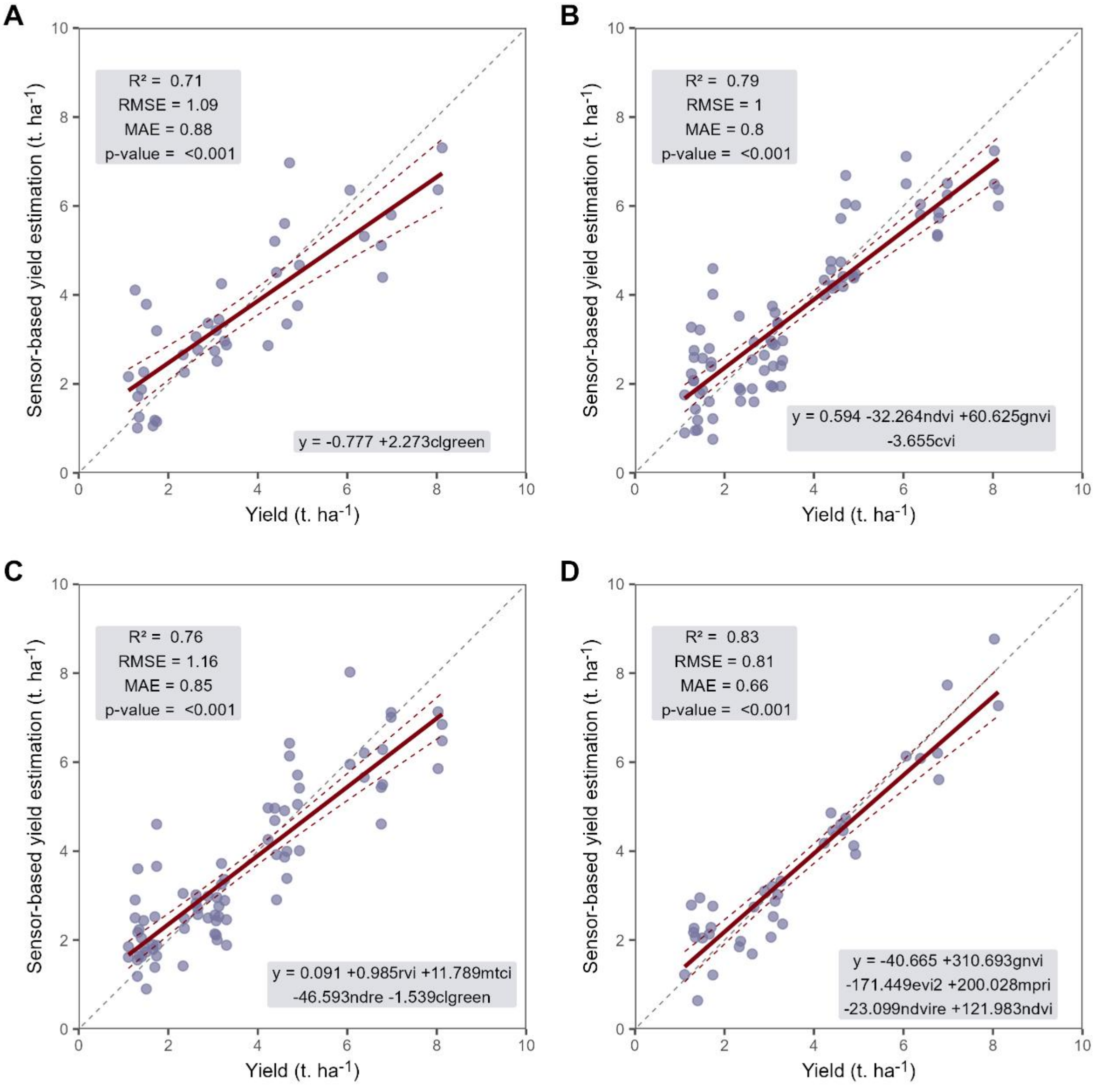

Such data and analysis justify the fact that sensors embedded in UAV are becoming one of the main tools for agricultural data acquisition, with great potential for a fast, accurate, efficient and economical reading of the most diverse agricultural parameters. In the present study, we were successful in estimating AGB, LAI, LNC and productivity, with promising results from the vegetative stage of the crop.

4. CONCLUSIONS

This study showed the ability of data collected by an Unmanned Aerial Vehicle (UAV) to estimate parameters related to nitrogen (N) content in the flooded rice crop. The growth stage was shown to have a significant impact on the performance of the various vegetation indices (IVs) assessed in estimating aerial biomass (AGB), leaf nitrogen content (LNC), leaf area index (LAI) and productivity. Initially, the data were split between the two cultivated rice varieties; however, the results indicated that the variety did not have a significant impact on the estimates, leading to the use of the two varieties together. This provides greater robustness and applicability of the models.

The simple models, using only one variable, such as NDVI or NDRE, demonstrated a good performance, both for the proximal Crop Circle sensor and for the use of UAV, with a superior efficiency for the data collected by UAV. However, the models often showed variations according to the phenological stages, suggesting a strong covariance effect, which limits the fit of linear models based on a single variable.

The results presented by the multiple linear regression models with multiple variables demonstrated good performance. All parameters, with the exception of productivity, obtained better estimates during the reproductive phenological stage, although promising results were also obtained when analyzing data from all stages. Yield was best estimated during the grain filling period. Data from UAVs represent a promising alternative as they overcome limitations caused by cloud cover that affect satellites. Additionally, they provide more comprehensive area coverage and require less operational time compared to ground-based optical sensors.

With the results of this study, rice producers (or analysts) can improve their decisions regarding nitrogen fertilization based on productivity forecasts throughout the cycle. Furthermore, given that only a small fraction of applied nitrogen is absorbed by plants, this efficient nitrogen management is crucial to mitigate losses to the environment and minimize impacts on greenhouse gas emissions.

This study underscores how the dependence on phenological stage and the susceptibility of spectral indices to saturation can influence nitrogen estimation, while also highlighting the promising future potential of expanding research to include validation in regions with distinct climatic conditions, soil properties, and management practices, alongside the exploration of additional sensor modalities to further enhance model robustness and applicability.

Conflict of interest

The authors declare no competing interests.

Data availability statement

The authors declare that the data supporting the findings of this study are available within the paper. Should any raw data files be needed in another format they are available from the corresponding author upon reasonable request. Source data are provided with this paper.

Funding statement

Gabriella Santos Arruda de Lima are CAPES research fellows (fellowships No. 001), Manuel Eduardo Ferreira (fellowships No. 317013/2023-8).

REFERENCES

Ali, A., Jabeen, N., Farruhbek, R., Chachar, Z., Laghari, A. A., Chachar, S., Ahmed, N., Ahmed, S., Yang, Z. Enhancing nitrogen use efficiency in agriculture by integrating agronomic practices and genetic advances. Frontiers in Plant Science., 2025 https://doi.org/10.3389/fpls.2025.1543714

Askari, M.S., McCarthy, T., Magee, A., Murphy, D.J. Evaluation of grass quality under different soil management scenarios using remote sensing techniques. Remote Sens. 11, 1–23, 2019. https://doi.org/10.3390/rs11151835

Bouguettaya, A., Zarzour, H., Kechida, A., Taberkit, A.M. Deep Learning Techniques to Classify Agricultural Crops through UAV Imagery: A Review. *Neural Comput. Appl.* **2022**, *34*, 9511–9536. https://doi.org/10.1007/s00521-022-07104-9

Brinkhoff, J.; Dunn, BW; Robson, AJ; Dunn, TS; Dehaan, RL Modelagem da absorção de nitrogênio no arroz no meio da temporada usando dados multiespectrais de satélite. Sensor Remoto 2019, 11, 1837. https://doi.org/10.3390/rs11151837

Broge NH & Leblanc E (2001) Comparing prediction power and stability of broadband and hyperspectral vegetation indices for estimation of green leaf area index and canopy chlorophyll density. Remote Sensing of Environment, 76:156-172. https://doi.org/10.1016/S0034-4257(00)00197-8 dos Santos M.P., Heinemann A.B., Stone L.F., da Matta D.H., de Castro J.R., dos Santos A.B. 2021. Nitrogen determination in irrigated rice using spectral reflectance. Agron. J. 113: 5087–5101. https://doi.org/10.1002/agj2.20892

Carracelas, G.; Hornbuckle, J.; Ballester, C. Monitoring Nitrogen Uptake and Grain Quality in Ponded and Aerobic Rice with the Squared Simplified Canopy Chlorophyll Content Index. *Remote Sens.* **2025**, *17*, 2598. https://doi.org/10.3390/rs17152598

Dash, J.; Curran, P. J. - The MERIS terrestrial chlorophyll index. International Journal of Remote Sensing. V. 25, 23, p. 5403-5413, 2004. 10.1080/0143116042000274015

Daughtry, C. S. T.; Walthall, C. L.; Kim, M. S.; de Colstoun, E. Brown; McMurtrey Iii, J. E. - Estimating Corn Leaf Chlorophyll Concentration from Leaf and Canopy Reflectance, Remote Sensing of Environment. V. 74, 2 p. 228-239, 2000. 10.1016/s0034-4257(00)00113-9

Equipe R. *R: Uma Linguagem e Ambiente para Computação Estatística*; R Foundation for Statistical Computing: Viena, Áustria, 2021; Disponível online: https://www.R-project.org/ (acessado em 1 de outubro de 2016).

Fageria, N. K.; dos SANTOS, A.B.; Stone, L. F. "Manejo de nitrogênio em arroz irrigado.", Circular técnica Embrapa, 58, 2003.

Fageria, N. K., & Baligar, V. C. Lowland rice response to nitrogen fertilization. *Communications in Soil Science and Plant Analysis*, *32*(9–10), 1405–1429, 2001. https://doi.org/10.1081/CSS-100104202

Frasson, F. R. Molin, J. P.; Salvi, J. V.; Povh, F. P.; Garcial, M. A. L. Utilização de sensor ótico ativo no diagnóstico de falhas de plantio em cana-de-açúcar. STAB, Piracicaba, v.26, n.2, p.34-37, 2007.

Fitzgerald, GJ; Rodrigues, D.; Christensen, LK; Belford, R.; Sadras, VO; Clarke, TR Sensoriamento espectral e térmico para o status de nitrogênio e água em ambientes de trigo irrigados e irrigados pela chuva. Precis. Agrícola 2006, 7, 233–248.

Gitelson, A. A.; Kaufman, Y. J.; Merzlyak, M. N. Use of a green channel in remote sensing of global vegetation from EOS-MODIS. Remote Sensing of Environment, v. 58, n. 3, p. 289–298, dez. 1996. https://doi.org/10.1016/S0034-4257(96)00072-7

Gong, Y., Yang, K., Lin, Z. et al. Estimativa remota do índice de área foliar (IAF) com imagens de veículos aéreos não tripulados (VANT) para diferentes cultivares de arroz ao longo de toda a estação de cultivo. Métodos de Planta 17, 88 (2021). https://doi.org/10.1186/s13007-021-00789-4

Gupta, SK; Pandey, AC Aspectos espectrais para monitoramento da saúde florestal em estações extremas usando imagens multiespectrais. *Egito. J. Remote Sens. Space Sci.* **2021**, *24*, 579–586.

Haboudane, D., Miller, J.R., Tremblay, N., Zarco-Tejada, P.J., Dextraze, L., 2002. Integrated narrow-band vegetation indices for prediction of crop chlorophyll content for application to precision agriculture, Remote Sensing of Environment, Vol. 81, 416–426, 2002. https://doi.org/10.1016/S0034-4257(02)00018-4

Han, S.; Hendrickson, L.; Ni, B. Comparison do satellite remote sensing and aerial photography for ability to detect in-season nitrogen stress in corn. ASAE Meeting, Paper n. 01-1142, 2001. https://doi.org/10.13031/2013.4120

Hartig, F. Dharma: Residual Diagnostics for Hierarchical (Multi-Level / Mixed) Regression Models2022. Disponível em: <https://cran.r-project.org/package=DHARMa>.

Huete, A. A soil-adjusted vegetation index (SAVI). Remote Sensing of Environment, v. 25, n. 3, p. 295–309, 1988. https://doi.org/10.1016/0034-4257(88)90106-X

Jiang, Z.; Huete, A.R.; Didan, K. Miura, T. Development of a two-band Enhanced vegetation index without a blue band. Remote Sensing of Environment. V.112, n.10, p.3833-3845, 2008. https://doi.org/10.1016/j.rse.2008.06.006

Jiang, XT; Gao, LT; Xu, X.; Wu, WB; Yang, GJ; Meng, Y.; Feng, HK; Li, YF; Xue, HY; Chen, TE Combinando sensoriamento remoto de VANT com aprendizado de conjunto para monitorar o conteúdo de nitrogênio foliar em pinha (*Annona squamosa* L.). *Agronomy* **2025**, *15*, 38.

Kuhn, M. Building Predictive Models in R Using the caret Package. Journal of Statistical Software, v. 28, n. 5, p. 1–26, 2008. https://doi.org/10.18637/jss.v028.i05

Lu, F., Sun, H., Tao, L., & Wang, P. (2025). Data Integration Based on UAV Multispectra and Proximal Hyperspectra Sensing for Maize Canopy Nitrogen Estimation. *Remote Sensing*, *17*(8), 1411. https://doi.org/10.3390/rs17081411

Li, M.H.; Liu, Y.; Lu, X.; Jiang, J.L.; Ma, X.H.; Wen, M.; Ma, F.Y. Integrating unmanned aerial vehicle-derived vegetation and texture indices for the estimation of leaf nitrogen concentration in drip-irrigated cotton under reduced nitrogen treatment and different plant densities. *Agronomy* **2024**, *14*, 120

Manes, Fausto; Anselmi, Silvia; Giannini, Monica; Melini, Susanna. Relationships between Leaf Area Index (LAI) and Vegetation Indices to analyse and monitor Mediterranean ecosystems. 328-335, 2001. https://doi.org/10.1117/12.413942.

Molin, J. P; Frasson, F. R.; Amaral, L. R.; Povh, F. P.; Salvi, J. V. Capacidade de um sensor ótico em quantificar a resposta da cana-de-açúcar a doses de nitrogênio. Revista Brasileira de Engenharia Agrícola e Ambiental, v.14, p.1345–1349, 2010. https://doi.org/10.1590/S1415-43662010001200014

Narmilan, A.; Gonzalez, F.; Salgadoe, A. S. A.; Kumarasiri, U. W. L. M.; Weerasinghe, H. A. S.; & Kulasekara, B. R. Predicting canopy chlorophyll content in sugarcane crops using machine learning algorithms and spectral vegetation indices derived from UAV multispectral imagery. Remote Sensing, 14(5), 1140, 2022. https://doi.org/10.3390/rs14051140

Niu, Y.; Zhang, L.; Zhang, H.; Han, W.; Peng, X. Estimating Above-Ground Biomass of Maize Using Features Derived from UAV-Based RGB Imagery. Remote Sens. 2019, 11, 1261. https://doi.org/10.3390/rs11111261

Peng, Y.P.; Zhong, W.L.; Peng, Z.P.; Tu, Y.T.; Xu, Y.G.; Li, Z.X.; Liang, J.Y.; Huang, J.C.; Liu, X.; Fu, Y.Q. Enhanced estimation of rice leaf nitrogen content via the integration of hybrid preferred features and deep learning methodologies. *Agronomy* **2024**, *14*, 1248

Pearson, R.L., Miller, L.D. Remote mapping of standing crop biomass for estimation of the productivity of the short-grass prairie, Pawnee National Grasslands, Colorado. In: Proceedings of the 8th International Symposium on Remote Sensing of Environment, ERIM International, pp. 1357–1381, 1972.

Qi, J. A.; Chehbouni, A.R.; Huete, Y.H.; Kerr, S.; Sorooshian, A modified soil adjusted vegetation index, Remote Sensing of Environment, Volume 48, Issue 2, 1994, Pages 119-126, ISSN 0034-4257. https://doi.org/10.1016/0034-4257(94)90134-1.

Rondeaux, G.; Steven, M.; Baret, F. Optimization of soil-adjusted vegetation índices Remote Sens. Environ., 107, pp. 95-107, 1996. https://doi.org/10.1016/0034-4257(95)00186-7

Rouse, J.W.; Haas, R.H.; Schell, J.A. et al. Monitoring vegetation systems in the Great Plains with ERTS. In: ERTS-1 SYMPOSIUM, 3., 1973, Washington. Proceedings... Washington: NASA, 1974. v.1, p.309-317.

Risso, J., Rizzi, R; Rudorff, B.F.T.; Adami, M.; Shimabukuro, Y.E.; Formaggio, A.R.; Epiphanio, R.D.V. Índices de vegetação Modis aplicados na área de áreas de soja. Pesquisa Agropecuária Brasileira, v. 47, p. 1317-1326, 2012. https://doi.org/10.1590/S0100-204X2012000900017

Segarra, J.; Rezzouk, FZ; Aparicio, N.; González-Torralba, J.; Aranjuelo, I.; Gracia-Romero, A.; Araus, JL; Kefauver, SC Avaliação multiescala de dados espectrais terrestres, aéreos e de satélite para monitoramento do teor de nitrogênio em grãos de trigo. *Inf. Process. Agric.* **2023** , *10* , 504–522.

Vincini, M.; Frazzi, E.; D'alessio, P. A broad-band leaf chlorophyll vegetation index at the canopy scale. Precision Agriculture, v. 9, n. 5, p. 303–319, 2008. . https://doi.org/10.1007/s11119-008-9075-z

Wang, Q.; Li, S.; Li, J.; Huang, D. **The Utilization and Roles of Nitrogen in Plants**. *Forests*, *15*, 1191, 2024. https://doi.org/10.3390/f15071191

Wu, W.F.; Li, X.Y.; Chen, S.C.; Jin, B.J.; Wu, C.Y.; Li, G.; Sun, C.L.; Zhu, Y.G.; Lin, X.Y. Nitrogen fertilization modulates rice phyllosphere functional genes and pathogens through fungal communities. *Science of The Total Environment*, v. 929, 2024. DOI: https://doi.org/10.1016/j.scitotenv.2024.172622.

Xu, D.; An, D.; Guo, X. The Impact of Non-Photosynthetic Vegetation on LAI Estimation by NDVI in Mixed Grassland. Remote Sens. 2020, 12, 1979. https://doi.org/10.3390/rs12121979

Xu, SZ; Xu, XA; Blacker, C.; Gaulton, R.; Zhu, QZ; Yang, M.; Yang, GJ; Zhang, JM; Yang, YA; Yang, M.; et al. Estimativa do conteúdo de nitrogênio foliar em arroz usando índices de vegetação e otimização de variáveis de características com fusão de informações de imagens de múltiplos sensores de UAV. *Remote Sens.* **2023**, *15*, 854.

Zambom, A.; Kim, J. New Algorithms and Software for Significance Controlled Variable Selection. Statistics, Optimization & Information Computing, v. 10, n. 3, p. 949–967, 2022.